Int. J. of GEOMATE, Dec, 2013, Vol. 5, No. 2 (Sl. No. 10), pp. 723-728
Geotec., Const. Mat. & Env., ISSN:2186-2982(P), 2186-2990(O), Japan

SIMULATING THE EFFECT OF FLOW VOLUME ON SCOURING PROCESS AROUND BREAKWATER UNDER TSUNAMI CONDITION BY SPH METHOD

M.R. Islam[1], K. Hayano[1] and A.M.K.N. Nadeesha[1]
[1]School of Urban Innovation, Yokohama National University, Japan

ABSTRACT: The study has attempted to simulate scouring process around the breakwater by smoothed particle hydrodynamics (SPH) method. SPH is a mesh less numerical method with a high capability of simulating large deformation of geo-material. However, SPH application in geotechnical problem is relatively new. The study has developed a simplified model arrangement with water and soil particle. Scouring process was simulated for saturated and dry soil by allowing water to fall continuously. The soil has the properties of elastic-perfectly plastic model with Mohr-Coulomb failure criteria. The water has the properties of viscous fluid. Scouring occurred as seepage force tried to drag the soil particles. Scouring process was found to advance with time and with increase in flow volume for both saturated and dry soil. The outcome of the study will help to predict the scour process around breakwater.

Keywords: SPH, Breakwater, Scour, Flow volume

1. INTRODUCTION

The Kamaishi seawall of 63 meters depth and 1,950 meters length was collapsed by the Great East Japan tsunami 2011. It was considered that scouring by the overtopping water had lowered the stability of the seawall foundation and caused to collapse. Scouring process consists of fluid movement and interaction with soil. To encounter such a complex problem Smoothed particle hydrodynamics (SPH) is very effective. SPH method is a particle method and does not require any mesh. A simplified 2D SPH model of water falling into the landward side of the breakwater is presented here. The study has attempted to simulate the behavior of scouring process by using the simple model. For developing the SPH code, the study has adopted the SPH theory written in Liu's book [1].

2. FUNDAMENTALS OF SPH

SPH is a particle method where the computational domain is discretized into a finite number of particles (or interpolating points). The material properties of a particle are evolved from the neighboring particles within support domain by using interpolation function. The interpolation process is based on the integral representation of a field function $f(x)$ follows:

$$\langle f(x)\rangle = \int_{\Omega} f(x)W(x-x',h)dx' \tag{1}$$

Where Ω is the area of the integration that contains x and x' ; and h is the smoothing length defining the influence domain of the smoothing kernel. $W(x-x',h)$ is the kernel or smoothing function, which must satisfy the following three properties: the first one is the normalization condition,

$$\int_{\Omega} W(x-x',h)dx' = 1 \tag{2}$$

The second condition is the delta function property that is observed when smoothing length approaches zero,

$$\lim_{h\to 0} W(x-x',h) = \delta(x-x') \tag{3}$$

Additionally, the third condition is the compact condition,

$$W(x-x',h) = 0, when\ |x-x'| > kh \tag{4}$$

Where k is a scalar defines the influence domain of the smoothing function.

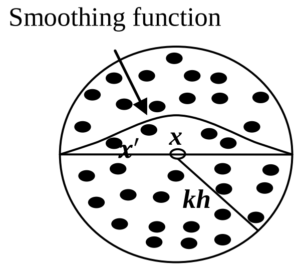

Fig. 1 Description of influence domain of a field variable 'x'.

There are many kernel functions but the study has used the cubic spline smoothing function. The cubic spline function was proposed [2]. The cubic spline function has the following form:

$$W(R,h) = \alpha_d \begin{cases} 1.5 - R^2 + 0.5R^3 & 0 \le R < 1 \\ \frac{(2-R)^3}{6} & 1 \le R < 2 \\ 0 & R \ge 2 \end{cases} \tag{5}$$

Where, $R = |x - x'|/h$, $\alpha_d = \frac{1}{h}, \frac{15}{7\pi h^2}, \frac{3}{2\pi h^3}$ respectively in one, two and three dimensions.

2.1 SPH formulations for fluid

The continuity equation used in the study is as follows:

$$\frac{\mathrm{D}\rho}{\mathrm{D}t} = \sum_{j=1}^{N} m_j \left(v_i^{\alpha} - v_j^{\beta}\right) \frac{\partial W_{ij}}{\partial x_i^{\alpha}} \tag{6}$$

Where, $\frac{\mathrm{D}\rho}{\mathrm{D}t}$ is the time derivative for density, m is mass, v is velocity ,$\frac{\partial W}{\partial x}$ is the first derivation of kernel, *i* is the first particle, *j* is the neighboring particle, *N* is the number of total neighboring particle , α and β are co-ordinate direction. Moreover, the momentum equation for each particle becomes

$$\frac{\mathrm{D}v_i^{\alpha}}{\mathrm{D}t} = \sum_{j=1}^{N} m_j \left(\frac{\sigma_i^{\alpha\beta}}{\rho_i^2} + \frac{\sigma_j^{\alpha\beta}}{\rho_j^2}\right) \frac{\partial W_{ij}}{\partial x^{\beta}} + g^{\alpha} \tag{7}$$

Where, σ is the total stress tensor, and *g* is the external force. Total stress σ for fluid is defined as

$$\sigma^{\alpha\beta} = -p\delta^{\alpha\beta} + \tau^{\alpha\beta} \tag{8}$$

Where, p is isotropic pressure, $\delta^{\alpha\beta}$ is the Kronecher's delta, $\tau^{\alpha\beta}$ is the viscous stress for fluid.

Isotropic pressure for fluid is obtained from equation of state.

$$p = B\left[\left(\frac{\rho}{\rho_0}\right)^{\lambda} - 1\right] \tag{9}$$

Where λ is a constant and set equal to 7 for most cases; ρ_o is the reference density; B is a problem dependent parameter, which sets a limit for the maximum change of the density. B *i*s usually chosen as $B = \frac{\rho_o c^2}{\lambda}$ where, c is the sound speed in water . However, to keep the density variation within 1% then $c = 10 v_{typ}$ is chosen.

For Newtonian fluids, the viscous shear stress should be proportional to the shear strain rate denoted by ε through the dynamic viscosity μ .

$$\tau^{\alpha\beta} = \mu\varepsilon^{\alpha\beta} \tag{10}$$

$$\varepsilon^{\alpha\beta} = \frac{\partial v^{\beta}}{\partial x^{\alpha}} + \frac{\partial v^{\alpha}}{\partial x^{\beta}} - \frac{2}{3}(\nabla \cdot v)\delta^{\alpha\beta} \tag{11}$$

2.2 SPH formulations for soil

SPH formulation for soil is similar with fluid with some exceptions. For soil the total stress is as follows:

$$\sigma^{\alpha\beta} = -p\delta^{\alpha\beta} + s^{\alpha\beta} \tag{12}$$

where σ is total stress, p is mean stress and s is deviatoric stress. However, deviatoric stress for the soil has been calculated from Hook's law as in the equation (13)

$$\frac{ds^{\alpha\beta}}{dt} = 2G\left(\dot{\varepsilon}^{\alpha\beta} - \frac{1}{3}\delta^{\alpha\beta}\dot{\varepsilon}^{\gamma\gamma}\right) + s^{\alpha\beta}R^{\beta\gamma} + s^{\gamma\beta}R^{\alpha\gamma} \tag{13}$$

Where, $\boldsymbol{G}$ is shear modulus, $\dot{\boldsymbol{\varepsilon}}$ is strain rate tensor, $\boldsymbol{R}$ is rotation rate tensor are defined as in Eq. (14), (15)

$$\dot{\varepsilon}^{\alpha\beta} = \frac{1}{2}\left(\frac{\partial v^{\alpha}}{\partial x^{\beta}} + \frac{\partial v^{\beta}}{\partial x^{\alpha}}\right) \tag{14}$$

$$R^{\alpha\beta} = \frac{1}{2}\left(\frac{\partial v^{\alpha}}{\partial x^{\beta}} - \frac{\partial v^{\beta}}{\partial x^{\alpha}}\right) \tag{15}$$

By combining Eq. (13), (14) and (15) the deviatoric shear stress components are calculated. According to the elastic-perfectly plastic soil model, the deviatoric stress components in the plastic region are scaled back to the maximum shear stress by the Mohr-Coulomb equation

$$s_{\mathrm{f}} = c + p\tan\phi \tag{16}$$

Where, c is the cohesion and p is the mean stress and $\boldsymbol{\phi}$ is the angle of internal friction. Mean stress of soil has been calculated as the Eq. (17)

$$p = K\left(\frac{\rho}{\rho_o} - 1\right) \tag{17}$$

Where, K is bulk modulus of soil. The study has taken the value of the K less than the actual as in the case of [4].

2.3 Soil-water interaction

In the preceding sections, SPH formulations for fluids and soils were described. However, it is needed how soil-water will interact with each other. The study has adopted the concept of two-phase flow for soil and water. When water will pass through the pores of the soils, it will exert drag force to the soil. This is called seepage force in soil. The seepage force acts on the soil particle and will be introduced into the momentum equation for soil and water as in [4], [5] .

$$f_{seepage} = \gamma_w n \frac{v_{water-v_{soil}}}{k} \tag{18}$$

where $\boldsymbol{\gamma}_{\mathbf{w}}$ is the unit weight of water, $\boldsymbol{n}$ is the porosity and $\boldsymbol{k}$ is permeability of soil.

2.4 Artificial viscosity

The artificial viscosity terms are usually added to the pressure term in the momentum equation to diffuse sharp variations in the flow and to dissipate the energy of high frequency. The study has used Monaghan type artificial viscosity $\prod_{ij}$. The detail formulation is as bellow:

$$\prod_{ij} = \begin{cases} \frac{-\alpha_{\prod} \ \bar{c}_{ij}\phi_{ij}}{\bar{\rho}_{ij}} & v_{ij}.x_{ij} < 0 \\ 0 & v_{ij}.x_{ij} \geq 0 \end{cases} \tag{19}$$

Where,

$$\phi_{ij} = \frac{\bar{h}_{ij}v_{ij}.x_{ij}}{|x_{ij}|^2 + 0.01\bar{h}_{ij}^2} \quad , \quad \bar{c}_{ij} = \frac{1}{2}(c_i + c_j)$$

$$\bar{h}_{ij} = \frac{1}{2}(h_i + h_j) \quad , \quad \bar{\rho}_{ij} = \frac{1}{2}(\rho_i + \rho_j)$$

In the above equations , $\alpha_{\prod}$, $\beta_{\prod}$ are constants

, in the study for water the values were taken as 0.01 and 0 respectively. However, for soil the values for the both were taken as 1.0.

With the inclusion of seepage force and artificial viscosity the momentum equation for soil is as follows:

$$\frac{\mathrm{D}_{v_i^\alpha}}{\mathrm{D}_t} = -\sum_{j=1}^{N} m_j \left(\frac{p_i^{\alpha\beta}}{\rho_i^2} + \frac{p_j^{\alpha\beta}}{\rho_j^2}\right)\frac{\partial W_{ij}}{\partial x^\beta} + \sum_{j=1}^{N} m_j \left(\frac{s_i^{\alpha\beta}}{\rho_i^2} + \frac{s_j^{\alpha\beta}}{\rho_j^2}\right)\frac{\partial W_{ij}}{\partial x^\beta} + g^\alpha + \sum_{j=1}^{N} m_j \left(\frac{f^{seepage}}{\rho_{water}\rho_{soil}}\right) W_{ip} \tag{20}$$

However, the momentum equation for water becomes as follow:

$$\frac{\mathrm{D}_{v_p^\alpha}}{\mathrm{D}_t} = -\sum_{q=1}^{N} m_q \left(\frac{p_p^{\alpha\beta}}{\rho_p^2} + \frac{p_q^{\alpha\beta}}{\rho_q^2}\right)\frac{\partial W_{pq}}{\partial x^\beta} + \sum_{q=1}^{N} m_q \left(\frac{\tau_p^{\alpha\beta}}{\tau_p^2} + \frac{\tau_q^{\alpha\beta}}{\tau_q^2}\right)\frac{\partial W_{pq}}{\partial x^\beta} + g^\alpha - \sum_{q=1}^{N} m_q \left(\frac{f^{seepage}}{\rho_{water}\rho_{soil}}\right) W_{ip} \tag{21}$$

In equation (21), p and q represent the first and second pair of the water particles. In the applications of the artificial compressibility to fluid flows, it is useful to use the 'XSPH' technique proposed by [2]. In the 'XSPH' technique fluid particle finally moves in the following way:

$$\frac{dx_p}{dt} = v_p - \varepsilon_{xsph} \sum_{q=1}^{N} \frac{m_q}{\rho_q} v_{pq} W_{pq} \tag{22}$$

Where, $\boldsymbol{\varepsilon_{xsph}}$ is a constant usually in the range of 0 to 1.0. The study has used 0.001 and found good result.

2.5 Boundary treatment

A SPH particle near or on the boundary while updating physical properties does not get neighboring particles from boundary side. This is called particle deficiency problem. The study has used symmetric image particles proposed by [3]. For each real particle located within kh distance from the boundary , an image particle is created symmetrically outside of the boundary. The image particle will have the same physical properties as the real one except the velocity and stress tensor. The velocity of an image particle normal to the boundary is taken as minus of the real one, in order to prevent the real particles from penetrating the boundary. However, velocity of an image particle tangent to the boundary is kept equal to the real one in order to simulate free-slip boundary condition on the symmetric plane. The stress tensor of an image particle is set according to the following relations:

$$\sigma_{image}^{\alpha\beta} = \begin{cases} \sigma_{real}^{\alpha\beta} & if\ \alpha = \beta \\ -\sigma_{real}^{\alpha\beta} & if\ \alpha \neq \beta \end{cases} \tag{23}$$

2.6 Time integration

Equation (6), (20) and (21) are integrated using a standard Leap-Frog (LF) algorithm with the following integration schemes:

$$\rho_{n+1/2} = \rho_{n-1/2} + \Delta t(\frac{D\rho}{Dt})_n \tag{24}$$

$$v_{n+1/2} = v_{n-1/2} + \Delta t(\frac{Dv}{Dt})_n \tag{25}$$

$$x_{n+1/2} = x_{n-1/2} + \Delta t(\frac{Dx}{Dt})_n \tag{26}$$

$$s_{n+1/2} = s_{n-1/2} + \Delta t(\frac{Ds}{Dt})_n \tag{27}$$

Where Δt is the time step; n indicates the current time t; and (n+1) indicates the advanced time (t+Δt). The Stability of LF scheme is guaranteed by several criteria for time step. The first one is the

Courant-Friedrichs-Levy(CFL) condition,

$$\Delta t \leq 0.25 \min \left(\frac{h}{c}\right) \quad (28)$$

And constraints due to the magnitude of particle acceleration f

$$\Delta t \leq 0.25 \min \left(\sqrt{\frac{h}{f}}\right) \quad (29)$$

And viscous diffusion

$$\Delta t \leq 0.125 \min \left(\frac{h^2}{v}\right) \quad (30)$$

Time step Δt for a simulation should be the minimum of value of Eq. (28)-(30).

3. DESCRIPTION OF NUMERICAL MODELS

A simplified model with a soil area of 0.095m X 0.25m was developed to simulated scouring process around the breakwater. Continuous water with discharges varying from 0.06m^3/m/s to 0.11m^3/m/s with falling heights of 0.01m was allowed to fall on the soil layer. Numerical simulations were done for the case of both saturated and dry soil. Saturated soil layer consists of both water and soil particle [4], [5] having the size of 0.005mX 0.005m. However, dry soil layer consists of soil particle only. The soil has the elastic-perfectly plastic properties with Mohr-Coulomb failure criteria. The elastic modulus of the soil was chosen as 20Mpa and Poisson's ratio was 0.3 with zero cohesion value. The density of soil was chosen as 1800 kg/m^3/m .The water was modeled as viscous fluid having dynamic viscosity of 10-^{3} Ns/m^2 and density 1000kg/m^3/m . Figure 2 depicts the initial arrangement of the simulation model.

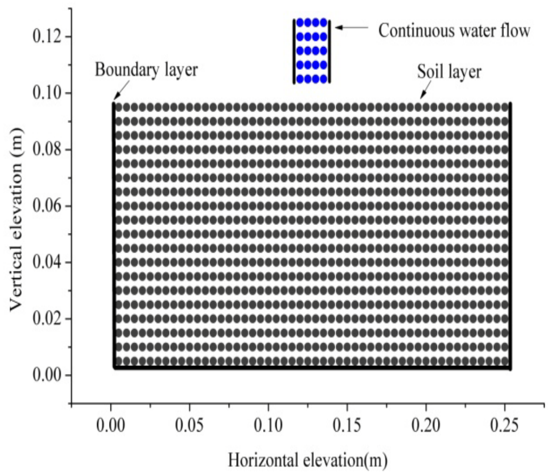

Fig. 2 Input condition of the simulation model.

3.1 Simulation results for saturated soils

Saturated soil was modeled as two-phase layer of water and soil [4], [5]. Although the soil and water stay closer but their physical properties will be governed by different system. The study has used two-phase model to allow the seepage force to work properly between water and soil. From Fig. 3 to Fig. 6 describe the progress of scouring process due to falling water. The particles in the saturated soil were found to show a little disturbance with the progress of simulation. This phenomenon may be related with excessive pore water pressure development. The study has used almost fifty percent of the saturated soil mass as the water particles. Figure 7 shows the progressive scouring depths with different flow volume with same fall height of 0.01m. It shows that with increase of flow volume scour depths increase.

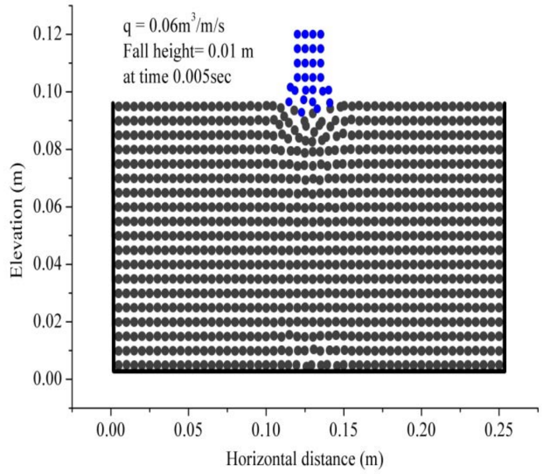

Fig. 3 Scouring progress of saturated soil at 0.005 seconds.

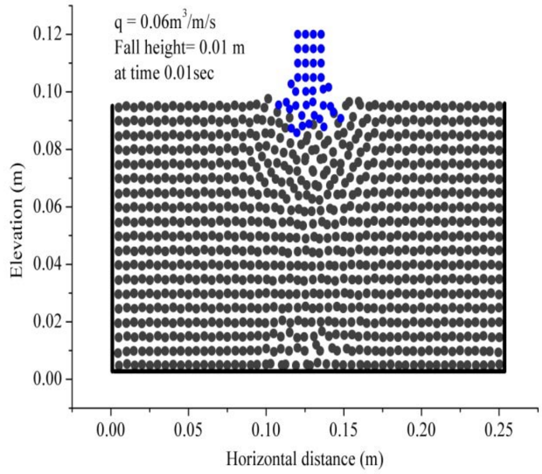

Fig. 4 Scouring progress of saturated soil at 0.01 second.

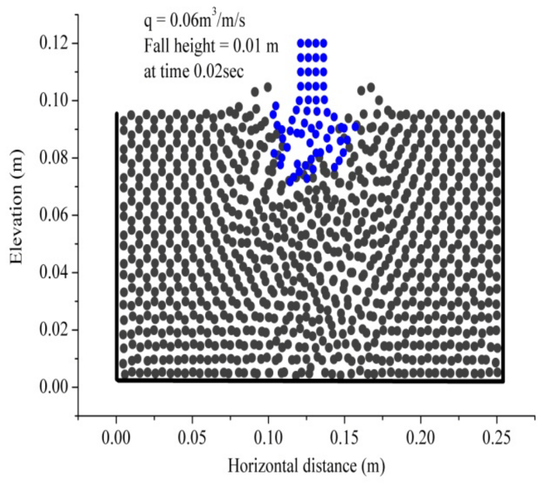

Fig. 5 Scouring progress of saturated soil at 0.02second.

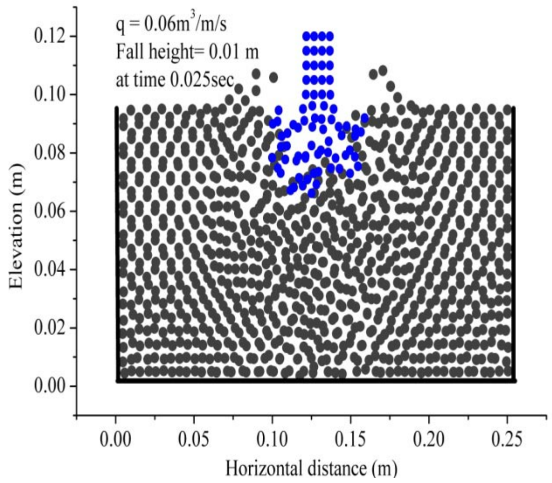

Fig. 6 Scouring progress of saturated soil at 0.025 second.

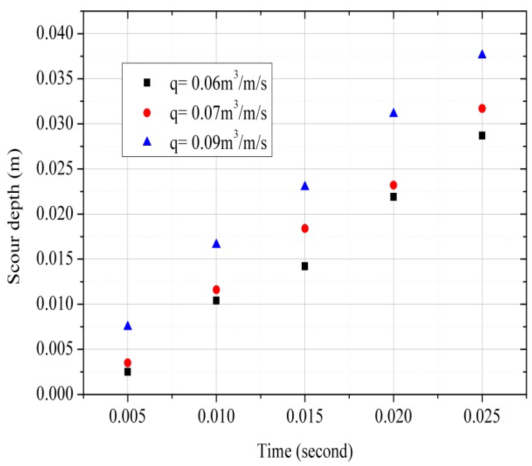

Fig. 7 Progressive scouring depths for saturated soil from 0.01m fall.

3.2 Simulation results for dry soils

Dry soil layer was modeled with the soil particles only. Fig.8, Fig.9, Fig.10 and Fig.11, show the progress of scouring process. However, it is observed that soil layer has the tendency of being compressed. As the soil layer follows the principle of continuum mechanics, and drag force by the water flow was considered in the momentum equation for soil, it shows some compressive behavior after being stressed by the drag force. Fig.12 shows that with the increase of flow volume scour depth increase. From Fig.7 and Fig.12, it is found that saturated soil shows large value of scour depth comparing with that of dry soil. It is because, in the study saturated soil has porosity filled with water. However, dry soil was considered more compacted than that of saturated soil.

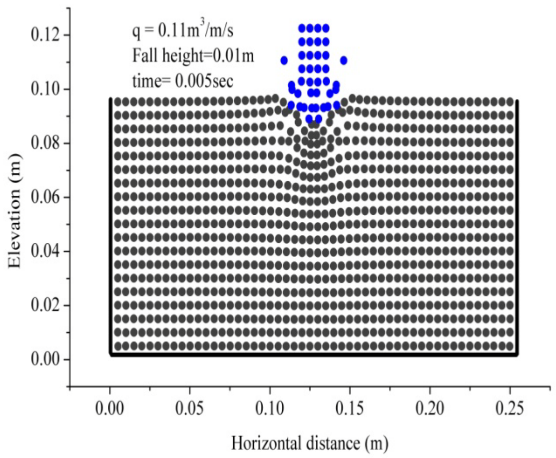

Fig. 8 Scouring progress of dry soil at 0.005second.

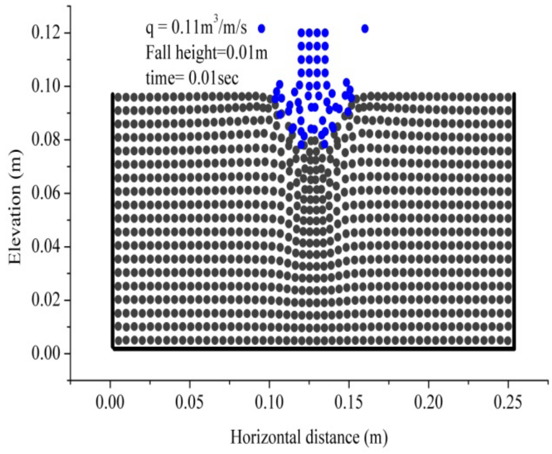

Fig. 9 Scouring progress of dry soil at 0.01second.

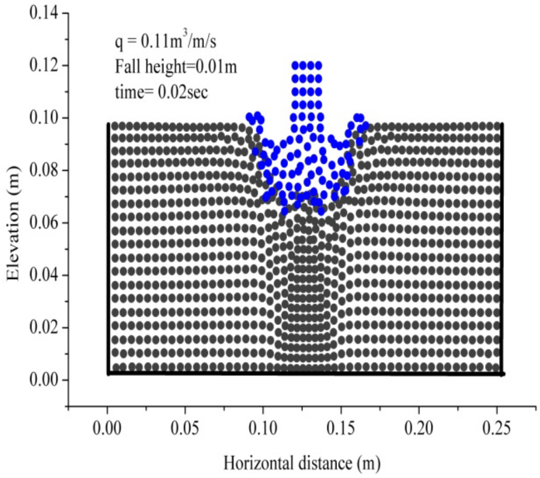

Fig. 10 Scouring progress of dry soil at 0.02second.

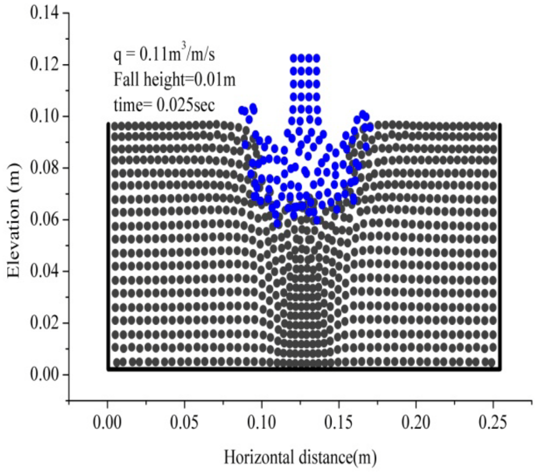

Fig. 11 Scouring progress of dry soil at 0.025second.

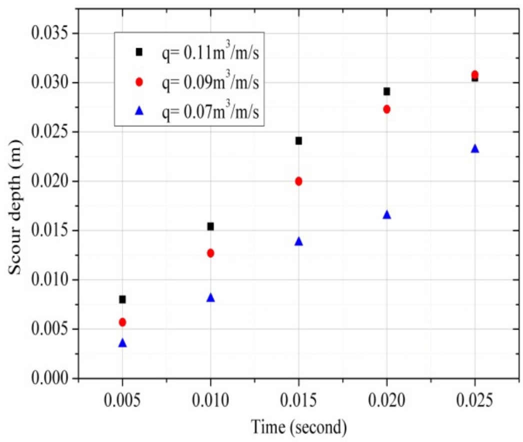

Fig. 12 Progressive scouring depths for dry soil from 0.01m fall.

4. CONCLUSION

The study has proved the capability of SPH method to simulate scouring process around breakwater in tsunami condition. In the simplified model, adopted here, saturated soil was modeled with water and soil particle. However, dry soil was modeled with only soil particle. It was found that scouring process progress with time and with increase of flow volume.

5. REFERENCES

[1] G.R. Liu and M.B. Liu, "Smoothed Particle Hydrodynamics; a meshfree particle method", World Scientific Publishing Co. Pte. Ltd. (2003)

[2] J.J Monaghan, "Simulating free surface flows with SPH", Computational Physics, Vol.110, (1994),pp 399-406.

[3] Libersky LD, Petschek AG, Carney TC et al., "High strain Lagrangian hydrodynamics: a three dimensional SPH code for dynamic material response. Journal of Computational Physics 1993; 109: pp.67-75.

[4] Bui Ha H., K. Sako and R. Fukagawa, "Numerical simulation of soil-water interaction using smoothed particle hydrodynamics (SPH) method", Journal of terramechanics 44 (2007) pp.339-346.

[5] Maeda Kenichi, Hirotaka Sakai and Mamoru Sakai, "Development of seepage failure analysis method of ground with smoothed particle hydrodynamics", JSCE vol.7, 2004, pp.775-786.

Int. J. of GEOMATE, Dec, 2013, Vol. 5, No. 2 (Sl. No. 10), pp. 723-728.
MS No. 3223 received on July 19, 2013 and reviewed under GEOMATE publication policies.

Pertinent discussion including authors' closure, if any, will be published in the Dec. 2014 if the discussion is received by June, 2014.
Corresponding Author: M.R. Islam